

NUCLEAR MAGNETIC RESONANCE PULSE APPARATUS

BY

Tsuneo HASHI, Akira HIRAI, Masahumi SASAKI and Takao KAWAI

(Received June 1, 1959)

ABSTRACT

A detailed description of the nuclear magnetic resonance pulse apparatus in our laboratory is given. This apparatus is intended for measuring the spin-lattice relaxation time of proton in high polymer between 10 msec and 1,000 msec.

1. Introduction

The nuclear magnetic resonance method has been used to give valuable informations about microscopic states and dynamical characters of many substances (1). Recently, the importance of informations about the spin-lattice relaxation time (T_1) has increased, particularly for high polymers, since the data obtained from nuclear magnetic resonance line width or line shape alone are not sufficient for full understanding of the internal motion in high polymer.

The saturation method (2), which has been most frequently used for the measurement of T_1 of high polymer, requires knowledge about the spin-spin relaxation time (T_2) and the magnetic rf field intensity (H_1). This method is rather complicated and there are further inconveniences caused by some anomalous phenomena associated with increasing magnetic rf field intensity (3, 4), particularly in solid. The pulse method (5) is relatively simple and direct. Thus, we have constructed a pulse apparatus for the purpose of measuring T_1 of proton in high polymer. This apparatus has been successfully operated except for samples in the rigid state which have broad lines and require, for measurement, extremely intense and narrow rf pulse and short receiver recovery time not realized in the present apparatus. This situation, however, is not serious for our present purpose, since the most interesting phenomena to be investigated for high polymers are about the internal motion and therefore the samples concerned are not in the rigid state.

Recently, a few articles have already appeared about the nuclear magnetic resonance pulse apparatus (6, 7). Still we feel it worth-while to report and discuss about our apparatus, because it is more convenient for measuring T_1 from 10 to 1,000 msec than other apparatus already reported, and in addition, it is difficult, in our

country, to use even some of the commercial devices described in the above articles, such as Tektronix Pulse Generator.

2. Construction of apparatus

The diagram of the whole apparatus is given in Fig. 1. We have adopted 90° - 90° pulse method for its simplicity of both construction and adjustment. The pulse train method is also applicable but was not adopted because of its critical dependence upon the 90° pulse setting. The T_1 of proton in high polymer is relatively long, so we have measured the pulse interval with a frequency counter consisting of a standard

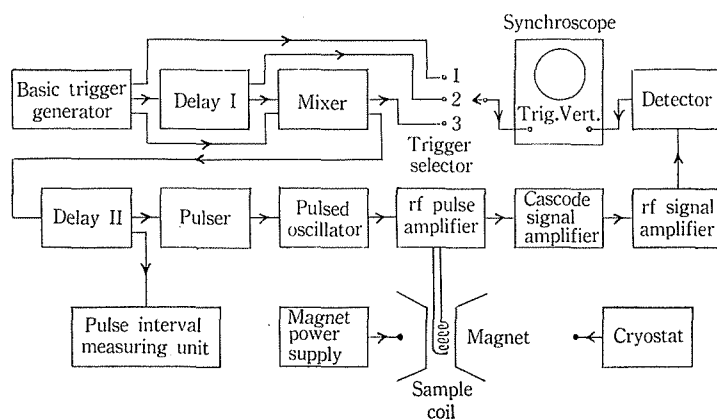


Fig. 1. Block diagram of the whole apparatus.

audio frequency oscillator, a bistable multivibrator, a gate and decatrons. Other units of the present apparatus are all of standard type as used in the ordinary pulse apparatus. Our measurements have been done at 25 Mc/sec and about 6,000 gauss. Each unit is described in detail in the following.

(1) Basic trigger generator

This unit determines repetition interval (the interval between basic triggers). The repetition interval should be very long compared with T_1 , while the shorter the repetition interval, the easier the measurement. In our measurement the repetition interval has been chosen between 0.5 and 5 sec. That the repetition interval is long enough has been ascertained by checking that the signal amplitude just after the first pulse (y_1) does not become larger for longer repetition interval. To obtain basic triggers, a frequency dividing unit and a decatron system were employed. The block diagram is shown in Fig. 2. Last three sections are inserted for eliminating undesired components of the output from the decatron, whose wave form consists of a desired large pulse, a long tail following and nine small pulses. The circuit diagram of the frequency dividing unit consisting of a cathode coupled monostable multivibrator (8) is shown in Fig. 3.

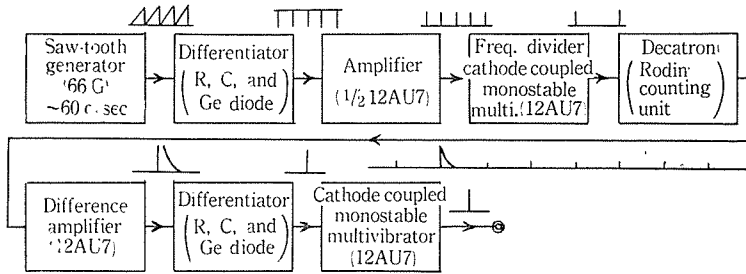


Fig. 2. Block diagram of basic trigger generator.

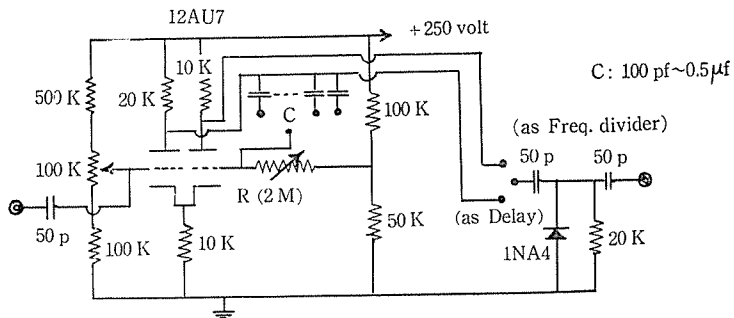


Fig. 3. Circuit diagram of cathode coupled monostable multivibrator as delay unit or as frequency dividing unit.

(2) Delay I

This is also a cathode coupled monostable multivibrator as in Fig. 3. This unit determines the pulse interval τ , which is the interval between the first and the second triggers and is measured by the pulse interval measuring unit.

(3) Mixer

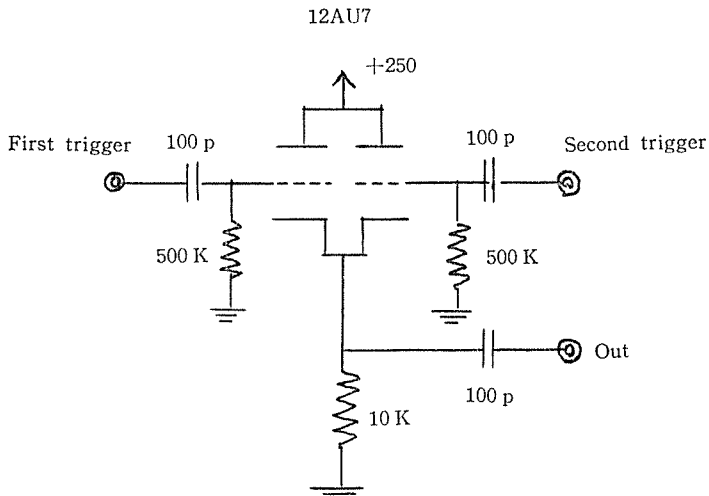


Fig. 4. Circuit diagram of mixer.

In this unit, the first and the second triggers are mixed. They are desired to have the same waveform. For this reason, the last section in the basic trigger generator (Fig. 2) is inserted. The circuit diagram is shown in Fig. 4.

(4) *Delay II*

This unit serves the signal being located at a desired position on the synchroscope screen. The circuit diagram is the same as in Fig. 3.

(5) *Pulser*

This unit is triggered by the output of Delay II and creates a rectangular waveform whose width (t_w) is controllable so as to be $\gamma H_1 t_w = \pi/2$ for 90° pulse. In our case, t_w was about $5\mu\text{sec}$ for 90° pulse. We have used a cathode coupled monostable multivibrator, though a more excellent circuit, such as plate coupled multivibrator with plate catching diode (9), would be desirable.

(6) *Pulsed oscillator*

A continuous rf oscillation and pulse modulation system (7) would be desirable for the frequency stability and the rf pulse wave shape. But it is very difficult to avoid the rf power leakage during off-time and this leakage makes beat with the nuclear signal, so we have adopted a pulsed oscillation system. This unit is essentially the same as that of E. L. Hahn (5). Care must be taken so that both the rf field intensity and the pulse width should not be modulated by heater hum voltage.

(7) *Pulsed rf amplifier*

This unit is inserted for obtaining a large rf magnetic field H_1 , which should be several times larger than the resonance line width $\Delta H_{1/2}$. In our apparatus, H_1 was about 15 gauss, which was limited not by the available power from power tube 813 but by rf pulse wave shape. We have lowered the "Q" of the sample coil to preserve good wave shape at the expense of rf field intensity. It is also desirable to set the rf amplifier, the sample coil, and the cascode signal amplifier in one chassis for avoiding the capacitive coaxial cable connections. The circuit diagram of this unit together with the sample coil is shown in Fig. 5.

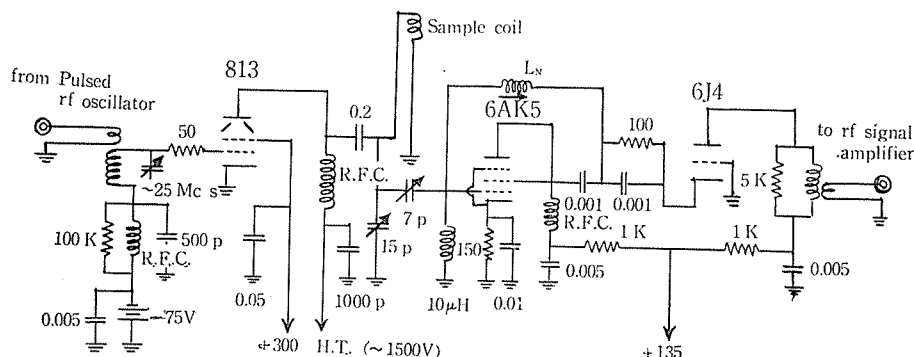


Fig. 5. Circuit diagram of rf pulse amplifier, sample coil, and cascode signal amplifier.

(8) *Cascode signal amplifier*

This unit serves for improving the overall S-N ratio, and is of original Wallman type (10). The circuit diagram is shown in Fig. 5.

(9) *rf signal amplifier and detector*

This unit is essentially of the standard type (11) with some modifications in the input stage. The circuit diagram of this unit is shown in Fig. 6. We have adopted the straight amplification system (gain 90 db, band-width 4 Mc/sec, receiver recovery time about 10 μ sec). But a superheterodyne system would be convenient in the

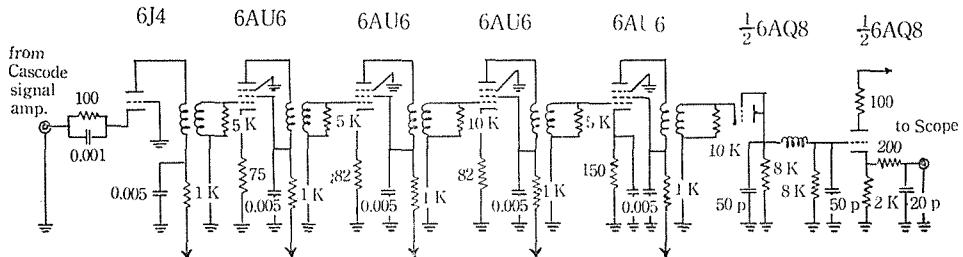


Fig. 6. Circuit diagram of rf signal amplifier.

variable rf frequency measurement. If the synchroscope has a good frequency characteristics up to about 30 Mc/sec, it is desirable to omit the detector to shorten the recovery time.

(10) *Synchroscope*

This is a commercial product. In our measurement, the signal appears on screen only once per several seconds, so a long persistent cathode ray tube or a memoriscope (recently commercialized) would be conveniently used.

(11) *Pulse interval measuring unit*

The block diagram of this unit is shown in Fig. 7. The audiofrequency oscillator is a commercial variable audio frequency oscillator, which is sufficient for our present purpose. For more accurate measurement, the crystal oscillator and frequency dividing system should be used. The circuit diagram of the bistable multivibrator (12) and

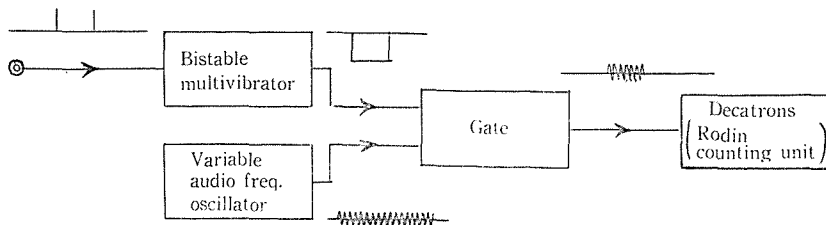


Fig. 7. Block diagram of pulse interval measuring unit.

the gate (13) is shown in Fig. 8. It may happen, however, that the decatrons begin counting the interval between the second and the next first triggers instead of the desired pulse interval. The switch in the diagram serves to change the measuring

from the undesired interval to the desired one.

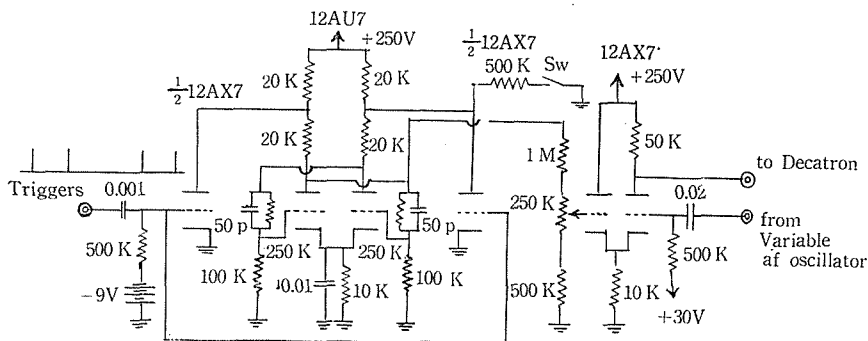


Fig. 8. Circuit diagram of bistable multivibrator and gate.

(12) Magnet

The diameter of pole piece is 12 cm. The pole gap is 3.6 cm. The current required for 6,000 gauss is about 500 mA. The field homogeneity is such that the free induction decay signal lasts about $500\mu\text{sec}$ for narrow lines, which was convenient for adjustment and measurement.

(13) Magnet power supply

This is essentially the same as that of H. L. Anderson (14). One measurement requires about 15 minutes, at least during which the dc magnetic field intensity (H_0) must be stable.

(14) Cryostat

A gas flow cryostat (15) has been used. The constancy of our apparatus was not so good, and about $\pm 1^\circ\text{C}$. We are now planning some improvements.

3. Procedures

(1) The dc magnetic field intensity H_0 is adjusted for exact resonance, searching for the maximum of the signal after the first pulse for a small pulse width t_w .

(2) Then, the pulse width is gradually expanded so as to satisfy 90° pulse condition, utilizing that the signal after the second pulse should be zero for a small pulse interval (Delay I) and 90° - 90° pulse condition (see Fig. 9 (a)). In Fig. 9 (a), the synchroscope trigger selector is set at 1 (in Fig. 1) and the synchroscope sweep speed is relatively low. With the trigger selector set at 3 (in Fig. 1) and the sweep speed increased, and otherwise on the same condition, the screen pattern is like Fig. 9 (b).

(3) Then the pulse interval is gradually expanded by changing R and C in Delay I, and calibrated by the pulse interval measuring unit (see Fig. 10). The difference between the signal after the first pulse y_1 and that after the second pulse (y_2) is plotted against the pulse interval τ on semi-logarithmic section paper. The slope of the plotted line, when straight, gives T_1 (see Fig. 11).

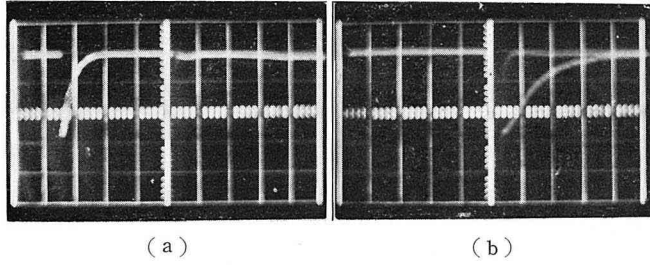


Fig. 9. Synchroscope screen pattern for $90^\circ-90^\circ$ pulse setting, second nuclear signal disappearing,
 Sample: PMA, Temperature: 34°C , Repetition interval: 2.2 sec,
 Resonance frequency: $\nu_0=25$ Mc/sec,
 Pulse width: $t_w=7\mu\text{sec}$,
 (a) Synchroscope trigger selector set at 1,
 Sweep rate: $200\mu\text{sec/cm}$,
 (b) Synchroscope trigger selector set at 3,
 Sweep rate: $50\mu\text{sec/cm}$.

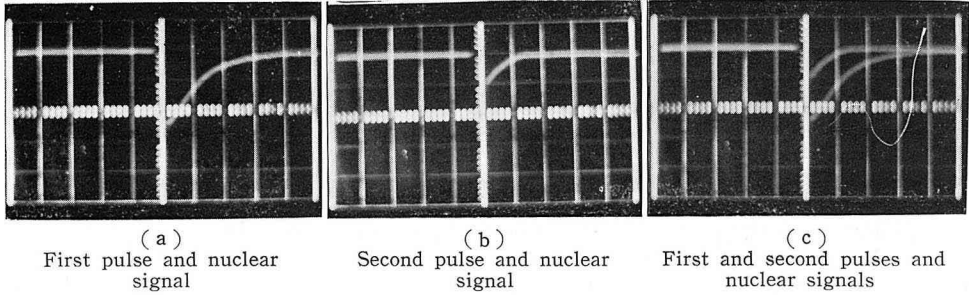


Fig. 10. Synchroscope screen patterns for measuring T_1 ,

Sample: PMA, Temperature: 34°C , Repetition interval: 2.2 sec,
 Resonance frequency: $\nu_0=25$ Mc/sec,
 Pulse width: $t_w=7\mu\text{sec}$,
 Sweep rate: $50\mu\text{sec/cm}$, Pulse interval: $\tau=140$ msec,
 (a) Synchroscope trigger selector set at 1,
 (b) Synchroscope trigger selector set at 2,
 (c) Synchroscope trigger selector set at 3.

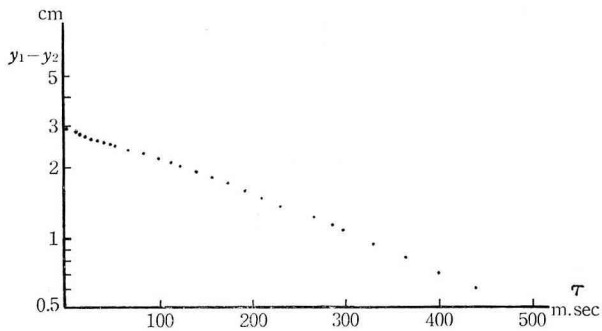


Fig. 11. Semi-logarithmic plot of difference between signal after first pulse (y_1) and that after second pulse (y_2) versus pulse interval τ , slope giving $T_1=290\text{msec}$. Data are given in Fig. 9.

The error of our measurement of T_1 is within about 10 per cent. It would come mainly from the reading error of the signal amplitude on the synchroscope screen. The failure in adjustment of 90° - 90° pulse condition and the fluctuations in the shape and width of the pulsed rf magnetic field cause also error, particularly in case of narrow intense pulses.

As mentioned in Introduction, the most important points for improvement to make the apparatus applicable to the sample in rigid state are to have a narrow intense rf pulse of good wave shape, and to have a short receiver recovery time. Both are very difficult to attain, though some efforts have been done (6, 7, 16, 17, 18). The present apparatus, however, is sufficient for investigating the internal motion in high polymer. The full data obtained by the present apparatus will be published later.

Acknowledgements

The authors would like to express their sincere thanks to Professor I. Takahashi for his continuous interest and discussion. The authors' thanks are also due to Mr. K. Sugibuchi and other members of our laboratory for their assistance.

REFERENCES

1. See, e.g. E. R. ANDREW, *Nuclear Magnetic Resonance* (Cambridge University Press, New York, 1955);
- G. E. PAKE, *Nuclear Magnetic Resonance* ('Solid State Physics' edited by F. SEITZ and D. TURNBULL Vol. 2, Academic Press New York, 1956) p. 1;
- M. H. COHEN and F. REIF, *Quadrupole Effects in Nuclear Magnetic Resonance Studies of* ('Solid State Physics' edited by F. SEITZ and D. TURNBULL Vol. 5, Academic Press Inc., New York, 1957) p. 321.
2. N. BLOEMBERGEN, E. M. PURCELL, and R. V. POUND, *Phys. Rev.*, **73** (1948), 679.
3. A. G. REDFIELD, *Phys. Rev.*, **98** (1955), 1786.
4. K. TOMITA, *Prog. Theor. Phys.*, **19** (1958), 541.
5. E. L. HAHN, *Phys. Rev.*, **80** (1950), 580.
6. J. SCHWARTZ, *Rev. Sci. Instr.*, **28** (1957), 780.
7. J. C. BUCHA, H. S. GUTOWSKY and D. E. WOESSNER, *Rev. Sci. Instr.*, **29** (1958), 55.
8. J. MILLMAN and H. TAUB, *Pulse and Digital Circuits* (McGraw-Hill Book Company, New York, 1956) p. 187 ff. and p. 363 ff.
9. Reference 8, p. 174 ff;
B. CHANCE, V. HUGHES, E. F. MACNICHOL, D. SAYRE and F. C. WILLIAMS, *Waveforms*, MIT Radiation Laboratory Series (McGraw-Hill Book Company, New York, 1949) p. 179 ff.
10. G. E. VALLEY and H. MILLMAN, *Vacuum Tube Amplifiers*, MIT Radiation Laboratory Series (McGraw-Hill Book Company, Inc., New York, 1948) p. 656 ff.
11. Reference 10, p. 166 ff.
12. Reference 8, p. 140 ff.
13. Reference 8, p. 435 ff.
14. H. L. ANDERSON, *Phys. Rev.*, **76** (1949), 1460.
15. E. L. ANDREW and R. G. EADES, *Proc. Roy. Soc.*, **A216** (1953), 398.
16. I. J. LOWE and R. G. NORBERG, *Phys. Rev.*, **107** (1951), 46.
17. I. SOLOMON, *Phys. Rev.*, **110** (1958), 61.
18. R. J. BLUME, *Phys. Rev.*, **109** (1958), 1867.